Crossref

GMPC

Research article

Metabolic plasticity of *Francisella tularensis* subsp. *holarctica* (wild type), *Francisella novicida* and *Francisella* sp. strain W12-1067

Thomas Steiner[1†], Fan Chen[2†], Kerstin Rydzewski[1], Clara Morguet[1], Felicia Achatz[1], Wolfgang Eisenreich[1*] and Klaus Heuner[2*]

[1] Bavarian NMR Center – Structural Membrane Biochemistry, Department of Chemistry, Technische Universität München, Garching, Germany

[2] Working group Cellular Interactions of Bacterial Pathogens, Centre for Biological Threats and Special Pathogens, ZBS 2, Robert Koch Institute, Berlin, Germany

Abstract

Francisella tularensis is a Gram-negative bacterium that causes a potentially fatal disease called tularemia. The highly infectious agent can spread via arthropod vectors, including ticks and via rodents such as rabbits or beavers. The facultative intracellular pathogen typically invades human macrophages at the onset of human infection. For intracellular replication of the bacteria, the usage of amino acids from the host cells and gluconeogenesis seem to be detrimental, but other carbon sources including glucose and glycerol are also utilized. Here, we compared the growth phase-dependent degradation of glucose, glycerol, and alanine in *F. tularensis* subsp. *holarctica* isolated from an infected beaver with the respective metabolism in the less virulent strains *F. novicida* strain U112 and *Francisella* sp. strain W12-1067. To this aim, we performed ^{13}C-labeling experiments with the bacteria growing in medium T supplemented with either [U-^{13}C$_6$]glucose, [U-^{13}C$_3$]glycerol, or [2,3-^{13}C$_2$]alanine during different growth phases. After cell harvest, mechanical disruption, and hydrolysis of cellular fractions, we determined the ^{13}C-profiles in various metabolites by mass spectrometry. The detected ^{13}C-patterns elucidated the metabolic fate of the supplied carbon nutrients and revealed minor, but significant differences indicative of various metabolic phenotypes of the *Francisella* strains under study. Glucose served as the main substrate for all strains under the experimental conditions. The sugar was degraded via the Embden-Meyerhof-Parnas pathway as the major catabolic route during growth. At lower rates, exogenous glycerol and alanine were used as co-substrates, particularly in the less pathogenic strains during the later growth phases. Our data support the hypothesis that, among other factors, the capability to adapt substrate usages efficiently and metabolic fluxes could determine the virulence of *Francisella* strains.

Keywords: *Francisella*, Intracellular bacteria, ^{13}C-Labeling, Isotopologue profiling, Metabolic adaptation, Tularemia

Introduction

Francisella tularensis is an intracellular Gram-negative bacterium, which infects a wide range of animals and humans (Ellis et al., 2002; Sjöstedt, 2011). In Germany, so far, only *F. tularensis* subsp. *holarctica* (*Fth*) could be identified as the causative agent of tularemia. *F. tularensis* subsp. *tularensis* (*Ftt*), being much more infectious than *Fth*, is mainly found in North America (Ellis et al., 2002; Appelt et al., 2020).

In 2014, a second *Francisella* species (*F.* sp. strain W12-1067 [F-W12]), isolated from the water reservoir of a cooling tower, was described to be present in Ger-

many (Rydzewski et al., 2014; Appelt et al., 2020). The F-W12 strain is negative for the classical *Francisella* pathogenicity island and seems to be less virulent. *F. novicida* (*Fno*) is less pathogenic for humans but highly pathogenic for mice. *Fno* is thought to be an opportunistic pathogen, infecting immune-compromised humans only (Siddaramappa et al., 2011). *Fno* strain U112 was originally isolated from water in Utah (Larson et al., 1955).

Many studies about *Francisella* were performed with the *Fth* strain LVS (live vaccine strain) since it is apathogenic for humans and its laboratory handling is

much easier. Here, we have investigated the *Fth* wild type (WT) strain A-271_1, freshly isolated from the carcass of a beaver deceased from tularemia (Schulze et al., 2016). The isolate was used without serial passaging on agar plates. Phylogenetically, this strain belongs to the B.12 subclade (biovar II, erythromycin resistant) of *Francisella* (Schulze et al., 2016; Appelt et al., 2019). The complete genome of this strain is known and displays genes for all classical virulence factors of *Fth* (Sundell et al., 2020). Notably, strains of biovar II are also frequently isolated from patients in Germany suffering from tularemia (Appelt et al., 2019).

Efficient replication of intracellular bacteria such as *Francisella* not only depends on special virulence factors but also on the metabolic adaptation of the bacterium to its host (cell) conditions (Eisenreich et al., 2010). Among *Francisella* species, diverse carbon substrates can be exploited for energy generation and anabolic demands (Gyuranecz et al., 2010; Huber et al., 2010; Chen et al., 2017). It was reported that glycolysis is dispensable for *F. tularensis* virulence, whereas gluconeogenesis is necessary for intracellular growth (Radlinski et al., 2018). Similar results were demonstrated for *Fth* and *Fno* (Brissac et al., 2015; Ziveri et al., 2017a,b). Indeed, glycerol was shown to serve as a substrate for intracellular *Ftt* and *Fno* (Brissac et al., 2015; Radlinski et al., 2018), but amino acids from the host are also important for intracellular replication of *Francisella*. These co-substrates are either catabolized to provide energy or used for gluconeogenesis (Barel et al., 2012; Gesbert et al., 2014; Ramond et al., 2014; Barel et al., 2015; Brissac et al., 2015; Gesbert et al., 2014, 2015; Ziveri et al., 2017a; Radlinski et al., 2018).

Under *in-vitro* conditions, the metabolism of *Francisella* is more diverse. It was shown that threonine, proline, methionine, lysine, tyrosine, tryptophan, asparagine, phenylalanine, alanine and serine improve growth in the absence of glucose, whereas glutamine, glutamate, leucine, isoleucine, histidine and arginine do not (Brissac et al., 2015). Indeed, *Fth* and *Fno* replicate well in Chamberlain's chemically defined medium (CDM) containing glucose as well as in the glucose-rich medium T (Brissac et al., 2015; Becker et al., 2016; Chen et al., 2017; Köppen et al., 2019). However, *Fno* and *F. tularensis* are unable to utilize glucose-6-phosphate since no glucose-phosphate transporter seems to be present in these strains (Gyuranecz et al., 2010; Huber et al., 2010; Gesbert et al., 2014; Ziveri et al., 2017b).

In addition, there seems to be no phosphotransferase system (PTS) system in *Fno* or *F. tularensis*, and it is still unclear which protein is responsible for the uptake of glucose in both species (Ziveri et al., 2017a). Thus, *Francisella* appears to be unable to directly use glucose-6-phosphate from the host cytosol (Ziveri et al., 2017b). Using a glucokinase mutant strain to support this hypothesis, we could demonstrate that F-W12 also lacks a functional PTS system. On the other hand, exogenous glucose within the medium highly improved the growth of this strain (Köppen et al., 2019). The same phenotype was also demonstrated for the intracellular growth of *F. tularensis* (Radlinski et al., 2018).

In earlier *in-vitro* ^{13}C-labeling studies, we could confirm that exogenous glucose serves as the major substrate for *Fth* and *Fno* (Chen et al., 2017). The observed ^{13}C-distribution in metabolic products revealed that the sugar is metabolized mainly through the Embden-Meyerhof-Parnas (EMP) pathway. We could also show that, next to glucose, glycerol is consumed as a co-substrate from the medium. The labeling patterns reflected that glycerol is converted into acetyl-CoA as a substrate for the TCA cycle, but it also serves as a gluconeogenetic precursor in *Fno*, and at lower rates also in *Fth* (Brissac et al., 2015; Chen et al., 2017; Ziveri et al., 2017b; Radlinski et al., 2018). This co-substrate usage suggested a bipartite metabolism in *Francisella*, similar to the earlier ones described for *Legionella pneumophila* and other pathogens (Grubmüller et al., 2014; Eisenreich et al., 2015; Gillmaier et al., 2016; Chen et al., 2017, 2020).

For better understanding of the dynamics in substrate usages of different *Francisella* strains, we here report *in-vitro* ^{13}C-labeling experiments during different growth phases, namely during (i) the exponential growth phase, (ii) the late-exponential/post-exponential phase, and (iii) the stationary phase. To this aim, the bacteria were grown in medium T (Becker et al., 2016) either containing [U-^{13}C$_6$]glucose, [U-^{13}C$_3$]glycerol, or [2,3-^{13}C$_2$]alanine as tracers. To specifically address the question of how virulence and pathogenicity are connected to substrate usages and metabolism, we compared the highly pathogenic *Fth* WT strain (A-271_1; "beaver isolate") (Schulze et al., 2016) with the *Fno* strain U112 (less pathogenic for humans) and the environmental aquatic *F.* sp. isolate W12-1067 (F-W12) (Rydzewski et al., 2014). To determine differences in the incorporation rates and the metabolic routes of the labeled supplements, we compared the ^{13}C-excess values and isotopologue profiles in multiple metabolites, e.g. in amino acids and cell wall sugars.

Material and Methods

Strains, growth conditions, media, and buffers

Strains used in this study were *Fth* wild type strain [isolate A-271_1; (Schulze et al., 2016)], *Fno* strain U112 [ATCC 15482; (Larson et al., 1955)] and *Francisella* sp. strain W12-1067 (Rydzewski et al., 2014). *Francisella* strains were cultivated at 37°C in medium T (Becker et al., 2016) containing 1% brain heart infusion broth (Difco Laboratories, Inc., Sparks, MD, USA), 1% bacto tryptone (Difco), 1% technical casamino acids (Difco), 0.005 g of MgSO$_4$, 0.01% FeSO$_4$, 0.12% sodium citrate, 0.02% KCl, 0.04% K$_2$HPO$_4$, 0.06% L-cysteine and 1.5% glucose.

Labeling experiments

One liter of growth medium (medium T) was supplemented with either 2 g of [U-^{13}C$_6$]glucose (11 mM), 0.46 g of [2,3-^{13}C$_2$]alanine (5 mM), or 2.5 g of [U-^{13}C$_3$]glycerol (25 mM), respectively (Eurisotop,

Saarbrücken, Germany). Volumes of 250 ml of supplemented medium T were inoculated with 20-40 ml of an over-night culture of the *Francisella* strains. Incubation was carried out at 37°C and 250 rpm. The optical density at 600 nm (OD600) was determined at regular intervals. Labeling experiments were done during the exponential (E), late/post-exponential (LE/PE), and stationary (S) phases, as indicated in Figure 1a. Before harvesting, a culture aliquot was plated onto lysogeny broth (LB) agar (Bertani, 1951, 2004) to rule out the possibility of contamination. At the end of each respective growth phase, the bacteria were pelleted at 4,700 g and 4°C for 15 min. The supernatant was discarded. The bacterial pellet was washed once with PBS and autoclaved at 120°C for 20 min. The pellet was resuspended in 4 ml of water and lyophilized.

In a control experiment, the concentration of free alanine, glucose, and glycerol in the supernatant was measured as described below after incubation of the strains at the start point, after the E phase and after the LE/PE phase in medium T. These values indicate the amount of free unlabeled substrates at the time points of the addition of labeled substrates which were subsequently used to determine the multiplication factors to normalize the mol% incorporation values of the labeled substrates (glucose, glycerol, alanine).

Workup of *Francisella* cells

Analysis of *Francisella* cell pellets was performed as described earlier (Chen et al., 2017). In brief, the lyophilized cell pellet was used to extract cytosolic metabolites, including free fructose. Proteins, cell wall or acid-labile polysaccharides were hydrolyzed, and amino acids, bound glucose from glycogen and glucosamine were isolated from the respective hydrolysates. The metabolites were subsequently derivatized and analyzed by GC-MS to determine ^{13}C-incorporation, as described earlier (Chen et al., 2017). Each experiment was performed twice, and each GC-MS sample was analyzed in three technical replicates. The results given below represent mean values and standard deviations, using six values for each metabolite under study (Tables S1-S27).

Analysis of the *Francisella* growth media

Analysis of *Francisella* growth media was performed as described earlier (Chen et al., 2017). In brief, after 0/5/15 h of growth (*Fno* and F-W12) or 0/10/25 h in the case of *Fth*, 1 mL of the supernatant was used for analysis with norvaline (5 mM) as an internal standard. Metabolite quantification was done via GC-MS. Each experiment was performed twice, and each GC-MS sample was analyzed in three technical replicates. Therefore, the results given below represent mean values and standard deviations using six values.

Results

### Growth phase characterization in *Fth*, *Fno*, and F-W12 strains

At first, we investigated the growth curves of *Fth* A-271 ("beaver isolate"), *Fno* U112 and F-W12 in medium T at 37°C. We chose the *Fth* wild type strain for the comparative study since the highly virulent strain could

allow correlating metabolism with virulence in comparison to the apparently less virulent strains under study. We observed a slower replication phenotype and delayed growth of *Fth* A-271 in medium T (Figure 1a). Notably, this slower replication resulting in delayed growth could not be observed for *Fth* strain LVS (data not shown). However, we could demonstrate previously that the general carbon flux in *Fth* LVS is similar to that of *Fth* strain A-271 *in-vitro* (Chen et al., 2017).

The prolonged E/PE phase of *Fth* A-271 was also considered for the time settings in the experiments with ^{13}C-labeled substrates. In Figure 1a, the time intervals of the respective growth phases (exponential phase [E], late exponential to post-exponential phase [LE/PE], and stationary phase [S]) are indicated. The ^{13}C-labeled substrates were added to the medium at the start of each phase, respectively. The unexpected slight raise of OD600 values detected for *Fno* after 25 h of growth were not correlated to bacterial growth as there was no increase of CFU values detectable for *Fno* during this growth phase (data not shown). In contrast, for the raise of OD600 values from 20 to 30 h for strain *Fth* A-271, also increasing CFU values could be observed (data not shown).

Using a glucokinase mutant strain of F-W12, we demonstrated in previous research that glucose has a positive effect on the growth of this strain during the late replicative phase (Köppen et al., 2019). To investigate if this also holds true for *Fth* and *Fno*, we performed growth experiments using medium T [MT (15 g glucose per L)] and medium T without glucose (MT-Glc) (Figure 1b). Indeed, the positive effect of glucose on growth was visible during the late to post-exponential phase for all three strains under investigation, but for *Fth*, a slight increase in bacterial growth was already detected in the E phase of growth (Figure 1b). Therefore, and as a control for the labeling experiments, we also determined the concentrations of free glucose, alanine, and glycerol in the supernatants of the three *Francisella* strains grown in medium T at the starting point of the experiment (0 h), the end of E phase (5 h/10 h) and the end of the LE/PE phase of growth (15 h/25 h) (Table 1).

Glycerol was not detectable except for the medium of *Fth* after 25 h of growth, albeit at a low concentration of 1.4 mmol l^{-1}. The concentration of free alanine slightly increased over time (F-W12>>*Fno*>*Fth*). Interestingly, despite the presence of a high concentration of free glucose (75 mM) in medium T at 0 h, the concentrations of free glucose in the supernatants of *Fno* and F-W12 slightly increased during the E phase and then decreased again, whereas, for *Fth*, the amount of glucose generally decreased over time. This suggested that glucose is used as an early substrate in *Fth* compared to *Fno* or F-W12, which agrees with the differences mentioned above between the three strains regarding the growth enhancement due to glucose (Figure 1b). The amounts of free, unlabeled glucose, alanine, and glycerol in the supernatant were further used to normalize the ^{13}C-mol% values of metabolites in the labeling ex-
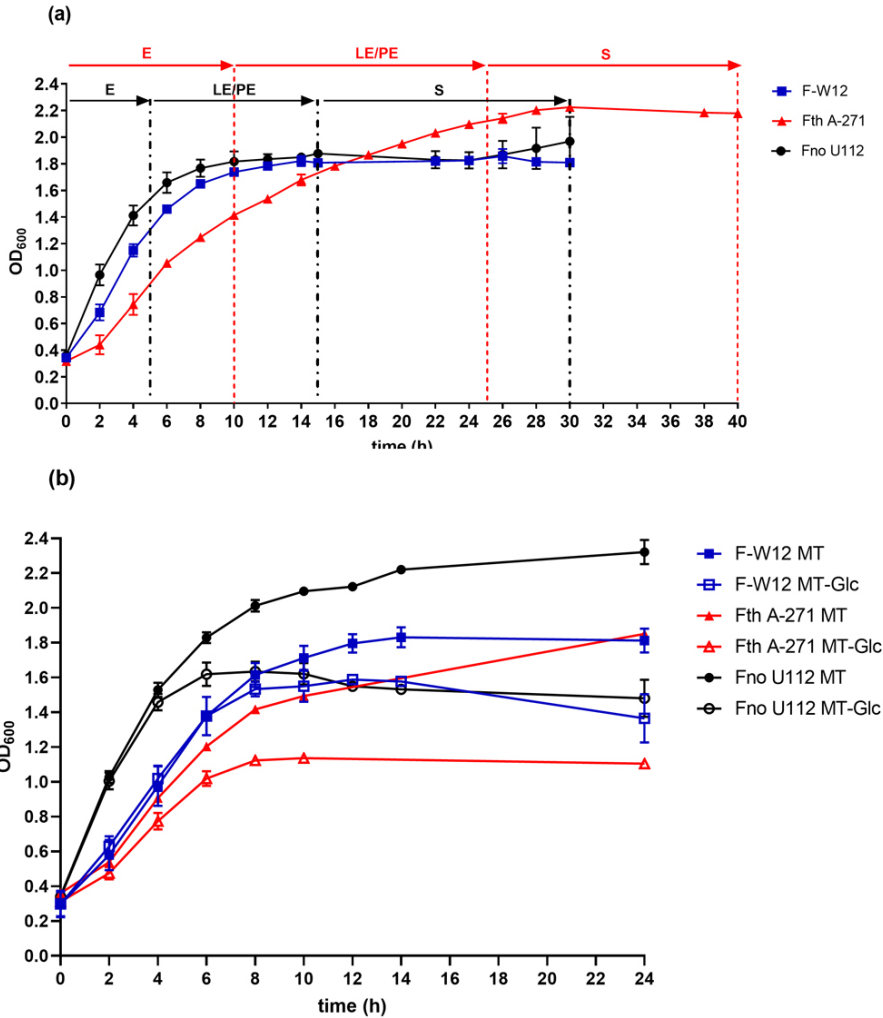
Figure 1: Growth behavior of the different *Francisella* strains under study. (a) Growth of *Francisella novicida* (*Fno* U112), *Francisella tularensis* subsp. *holarctica* (*Fth* A-271), and *Francisella* F-W12 (F-W12) in medium T. Results are mean values with standard deviations of three independent experiments. Bacterial cells were harvested at the exponential (E), late-exponential/post-exponential (LE/PE), and stationary (S) phases of growth. Time periods of the ^{13}C-labeling experiments for *Fno* U112, F-W12 (black arrows), and *Fth* A-271 (red arrows) are indicated. (b) Growth of *Fno* (*Fno* U112), *Fth* (*Fth* A-271), and F-W12 (F-W12) in medium T with (MT) and without (MT-Glc) glucose was investigated at different time points over 24 h of incubation. Results are mean values and standard deviations of three independent experiments.

periments with respect to the ratio between unlabeled and labeled substrates in the medium. Therefore, the different substrates are directly comparable in terms of their relative usage rates, and the values mentioned below refer to these normalized ^{13}C-excess values in the respective metabolite.

Comparative ^{13}C-isotopologue profiling analysis

In earlier work, we analyzed the metabolic capabilities of *Fth* and *Fno* through isotopologue profiling using ^{13}C-glucose, ^{13}C-glycerol as well as ^{13}C-serine as tracers. Herein, a general metabolic model could be established based on ^{13}C-incorporation and isotopologue distributions (Chen et al., 2017). The same metabolic model now served for data analysis to reveal the metabolic pathways under the various conditions.

For analysis of the metabolic fluxes, different classes of metabolites were analyzed. Mechanical disruption of the cells allowed direct analysis of cytosolic, un-bound

metabolites, while chemical lysis yielded data for cell-wall-bound sugars and protein-bound amino acids.

F. tularensis subsp. *holarctica* WT

Figure 2 represents the simplified metabolic scheme for growth phase-dependent substrate usages in *Fth*. In the scheme, Figure 2a summarizes the carbon fluxes from exogenous [U-^{13}C$_6$]glucose, Figure 2b from exogenous [U-^{13}C$_3$]glycerol, and Figure 2c from exogenous [2,3-^{13}C$_2$]alanine, respectively.

In general, the C3-compounds, glycerol, alanine, and lactate, derived from the glycolytic intermediates, glyceraldehyde phosphate, and pyruvate, respectively, displayed significant ^{13}C-incorporation from the supplied [U-^{13}C$_6$]glucose (glycerol, 66 to 36%; alanine, 64, 75 and 51%; lactate, 41 to 13%, Figure 2a, Tables S10-S12). Their isotopologue profiles were dominated by M+3 labeling, i.e., reflecting three ^{13}C-labels in the metabolites (data not shown). Additionally, the pres-

Table 1: Concentrations of unlabeled alanine, glycerol, and glucose [mM] in the supernatant during different time points of *Francisella* growth in medium T as determined by GC-MS. 0 h represents the start of the exponential growth phase, 5 h/10 h represents the beginning of the late/post-exponential growth phase, and 15 h/25 h represents the beginning of the stationary phase (Figure 1a). Values are given as means of two biological replicates with three technical replicates each. [#]Values were taken from an earlier work under similar conditions (Chen et al., 2017).

Strain	Time	Concentration [mM]		
		Alanine	**Glycerol**	**Glucose**
F. tularensis* subsp. *holarctica	0 h	0.4[#]	0[#]	75.3[#]
	10 h	2.6	0	55.3
	25 h	4.6	1.4	28.4
F. novicida	0 h	0.4[#]	0[#]	75.3[#]
	5 h	0.8	0	95.4
	15 h	4.9	0	45.7
***Francisella* sp. strain W12-1067**	0 h	0.4[#]	0[#]	75.3[#]
	5 h	3	0	101.1
	15 h	11.5	0	68

ence of M+1 and M+2 labeling in alanine and lactate suggested active decarboxylation of a C4-intermediate (with M+1 and M+2 labeling) from the TCA cycle, e.g., via PEP carboxy-kinase, malate dehydrogenase, or aspartate 4-decarboxylase.

The production of labeled acetyl-CoA was reflected by the ^{13}C-excess and isotopologue profiles of the fatty acids, palmitate, and stearate (38 and 29% ^{13}C-incorporation, respectively). Labeled acetyl-CoA also entered the TCA cycle, leading to ^{13}C-incorporation into the TCA intermediates, α-ketoglutarate resp. glutamate (25, 20, and 9%) as its direct transamination product and succinate (13, 32, and 17%). Notably, all TCA cycle-related intermediates and products displayed significant ^{13}C-excess and diverse isotopologue profiles (Tables S10-S12) arising through the propagation of the acetyl-CoA moiety via the TCA cycle and eventual combination of labeled precursors in the citrate synthase reaction. For a detailed interpretation of the labeling profiles, see also (Chen et al., 2017).

The analysis of hexose sugars (i.e., of detected glucose, fructose, and glucosamine) mostly resulting from hydrolysis of the cell wall revealed high ^{13}C-excess values through the incorporation of [U-[13]C$_6$]glucose during the E phase for cell wall-derived glucosamine (76%), free fructose (85%) and bound glucose (100%, Tables S10-S12, S19-S21). However, these sugars displayed diverse isotopologue profiles, not only reflecting the expected M+6 species (i.e., molecules carrying six ^{13}C-labels) but also showing lighter isotopologues (e.g., M+3), especially in glucosamine (data not shown). This was taken as evidence for active gluconeogenesis using M+3 and lighter labeled precursors. Together with the high ^{13}C-excess values, this suggested an active synthesis of cell wall sugars in the E phase.

In the LE/PE phase, glucose metabolization led to an increase in ^{13}C-excess in most metabolites except for sugars, glycerol, and lactate (Tables S1-S3,

S10-S12, S10-S12). The ^{13}C-excess in glucosamine and fructose decreased significantly from 76% to 40% and 85% to 58%, respectively (Figure 2a). However, TCA cycle intermediates, protein bound amino acids (alanine, glutamate, tyrosine, and aspartate), free alanine, and fatty acids showed a significant increase (Figure 2a). Additionally, isotopologue profiles of fatty acids displayed higher abundances of heavier isotopologues (data not shown). This suggested increased carbon flux from the supplied ^{13}C-glucose into acetyl-CoA, serving for fatty acid synthesis and the TCA cycle during the PE phase.

Interestingly, glutamate did not show this increased ^{13}C-incorporation, probably reflecting lower rates of de novo glutamate formation after the exponential growth phase. In the S phase, the ^{13}C-excess values using ^{13}C-labeled glucose generally decreased (Figure 2a). Thus, the carbon flux from glucose into metabolites in *Fth*, in general, was highest during the LE/PE phase of growth. [U-[13]C$_3$]glycerol was efficiently taken up, resulting in more than 87% (E), 86% (LE/PE), and 93% (S) of re-isolated cytosolic glycerol (Tables S13-S15). Nevertheless, the carbon flux from glycerol into other metabolites in *Fth* was 10 to 50 times lower than that utilizing glucose (Figure 2b), although similar isotopologue compositions were produced in the downstream metabolites as in the experiment with [U-[13]C$_6$]glucose (Tables S4-S6, S13-S15, S22-S24). This indicated that the supplied glycerol was shuffled into glycolysis as M+3 3-phosphoglycerate, which was also a key intermediate from glucose degradation.

There were also low but significant levels of ^{13}C-excess in glucosamine (1.4%) and fructose (0.8%), confirming active gluconeogenesis (Tables S22-S24). When comparing the labeling data during the different growth phases, glycerol usage was highest in the E phase of growth and then steadily decreased towards the S phase (Figure 2b).
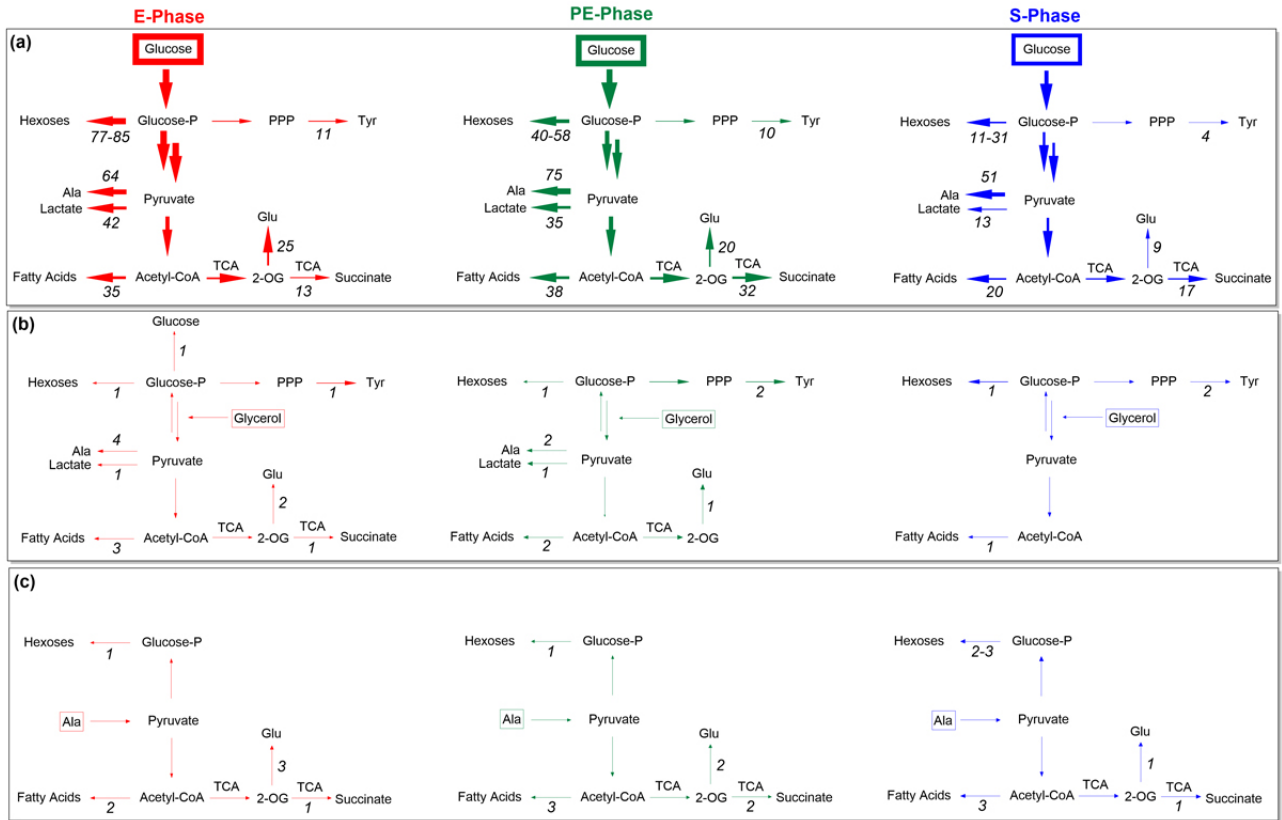
Figure 2: Overview of growth phase-dependent metabolization of (a) glucose, (b) glycerol, and (c) alanine in *F. tularensis* subsp. *holarctica* (*Fth*). Boxes indicate the supplied ^{13}C-labeled substrates. Red arrows represent metabolic fluxes in the early exponential growth phase, green arrows represent the late/post-exponential growth phase, and blue arrows represent metabolism during the stationary phase. The thickness of the arrows is proportional to the ^{13}C-incorporation into the respective metabolite (Tyr refers to protein-bound Tyr; hexoses include free fructose, bound glucose, and cell wall-derived glucosamine; the other metabolites were isolated from the cytosol), which is also indicated by relative fluxes in % below the arrows. Glucose-P: glucose-phosphate; PPP: pentose phosphate pathway; 2-OG: 2-oxoglutarate; TCA: tricarboxylic acid cycle.

In the experiments with [2,3-^{13}C$_2$]alanine, the ^{13}C data showed that the labeled amino acid was used directly for protein biosynthesis or that it was transformed to M+2 pyruvate and further downstream products (Figure 2c), although an alanine transaminase or dehydrogenase is not annotated in the genome of *Fth* (Ziveri et al., 2017b) (Tables S7-S9, S16-S18, S25-S27). Further reactions led to M+2 acetyl-CoA, which causes similar isotopologue distributions in fatty acids and TCA cycle-related metabolites as observed in the experiments with labeled glucose and glycerol, respectively.

Gluconeogenesis from alanine occurred only at very low levels but was highest in the S phase of growth (Tables S25-S27). The ^{13}C-excess of free alanine decreased over time, which may be due to the increasing amount of unlabeled alanine in the supernatant of *Fth* over the whole time, as observed through the analysis of the medium (Table 1).
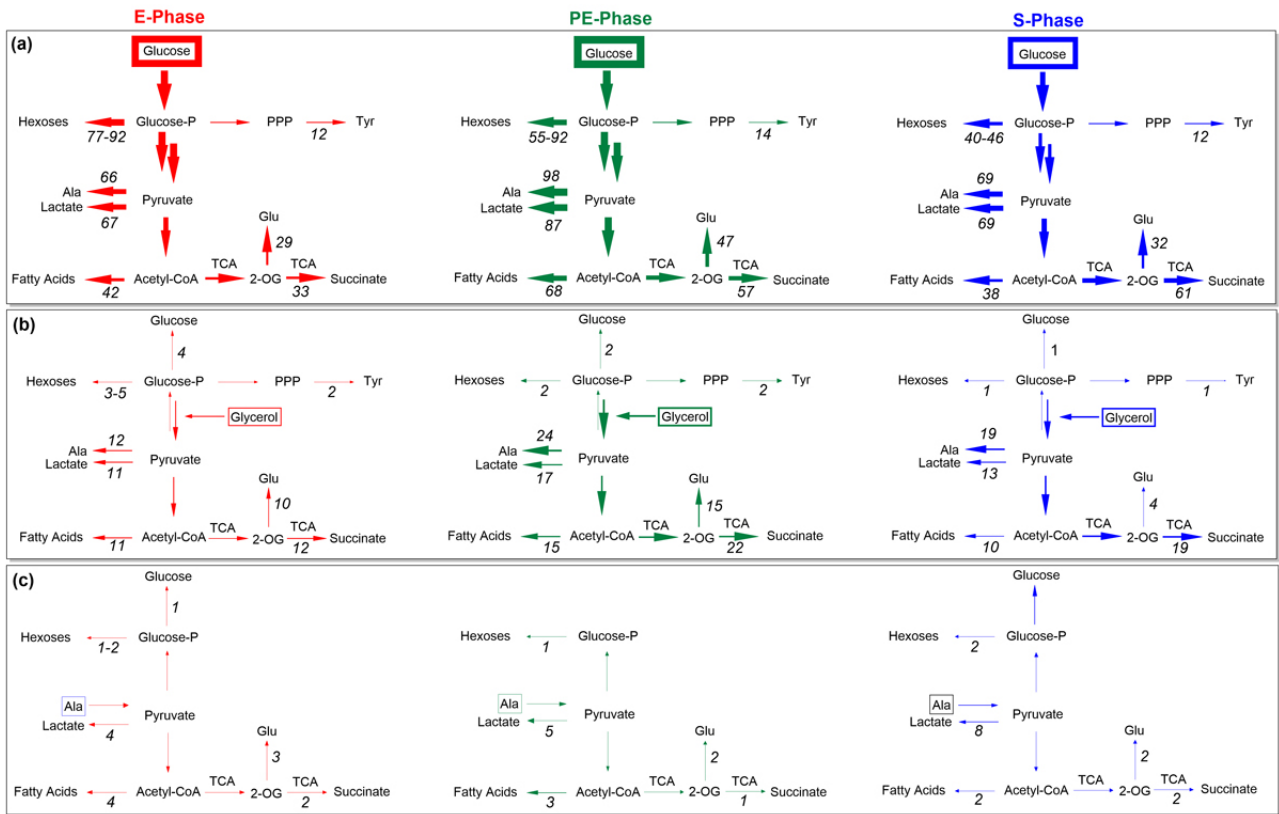
Francisella novicida

When feeding [U-^{13}C$_6$]glucose, *Fno* showed similar values and isotopologue distributions as *Fth* during exponential growth (Figure 3). However, it should be mentioned that the ^{13}C-excess values were generally

slightly higher (Tables S1-S3, S10-S12, S19-S21). Excess values were highest in fructose (92%) and glucosamine (77%), both showing indications for gluconeogenesis, despite high levels of glucose in the medium (Table 1).

In the LE/PE phase, glucose usage generally increased, especially leading to increased ^{13}C-incorporation into glycerol (94%), lactate (87%), and alanine (98%) which are directly derived from glycolytic intermediates (Tables S10-S12). Following this tendency, TCA cycle intermediates and acetyl-CoA-derived metabolites also showed increased ^{13}C-excess compared to the preceding growth phase (fatty acids [67%], succinate [57%], and glutamate [47%]). In general, glucose usage was highest in the LE/PE phase and decreased again in the stationary phase, as already described for *Fth*. [U-^{13}C$_3$]glycerol was metabolized similarly to glucose but at a substantially lower rate, especially for gluconeogenesis (Tables S4-S6, S13-S15, S22-S24). Still, excess values of 4.0% in glucose, 4.7% in glucosamine, and 2.8% in fructose during the E phase showed active gluconeogenesis from [U-^{13}C$_3$]glycerol in *Fno*.

In the post-exponential phase, glycerol usage increased significantly. Alanine and lactate showed al-

Figure 3: Overview of growth phase-dependent metabolization of (a) glucose, (b) glycerol, and (c) alanine in *Francisella novicida* (*Fno*). Boxes indicate the supplied ^{13}C-labeled substrates. For more details, see the legend of Figure 2.

most exclusively M+3 labeling with ^{13}C-excess values of 24% and 17%. In addition, in the PE phase, fatty acids (14%) were predominantly evenly labeled with similarly high ^{13}C-excess values. The high portion of M+2 acetyl-CoA also led to an enrichment of multiply labeled TCA cycle-related metabolites. The glycerol uptake in the stationary phase seemed to be highly reduced, leading to a decrease in the ^{13}C-excess of cytosolic glycerol from >80% to 49% during this phase (Tables S13-S15). Subsequently, the ^{13}C-excess values in all metabolites were lowered.

The ^{13}C-Incorporation from [2,3-^{13}C$_2$]alanine was again much lower than that from ^{13}C-glucose and ^{13}C-glycerol but, in contrast to these substrates, metabolization and especially gluconeogenesis decreased during the post-exponential growth and then increased in the S phase (Tables S7-S9, S16-S18, S25-S27). Notably, the ^{13}C-excess values in lactate were higher in all growth phases compared to *Fth*.

Francisella sp. strain W12-1067

Similar to the other strains, F-W12 showed efficient glucose usage via the pathways discussed before for *Fth* and *Fno* (Tables S1-S3, S10-S12, S19-S21). Nevertheless, the incorporation rates were lower in F-W12 for all metabolites under study (Figure 4a). During the post-exponential phase (PE), glucose utilization generally increased. Thus, glucose was used more intensively during the PE phase, leading to high excess values in glucosamine (52%), lactate (77%), fatty acids (43%), and TCA intermediates/products (succinate

70%, glutamate 24%). However, during the stationary phase, fatty acids showed reduced ^{13}C-incorporation, while TCA cycle-related metabolites revealed higher ^{13}C-excess values than those in the preceding growth phases.

Glycerol was taken up at a very high rate, resulting in a ^{13}C-excess of 92.5% for cytosolic glycerol in all three growth phases (Tables S13-S15). Subsequently, glycerol metabolization led to ^{13}C-incorporation similar to the rates observed for *Fno*. In the LE/PE phase, glycerol utilization generally increased, with gluconeogenesis being the only exception. Metabolites derived from pyruvate showed a constant increase over time (S phase: lactate 21%, free alanine 21%), while acetyl-CoA-derived metabolites showed more pronounced labeling in the LE/PE phase, followed by a decrease again during stationary growth. Gluconeogenesis from glycerol was highest in the E phase (Tables S22-S24). This declined over time but was still higher in F-W12 during all growth phases when compared to *Fth* or *Fno*.

Alanine was also taken up and utilized by F-W12 during all growth phases at higher rates than in *Fth* or *Fno* (Tables S16-S18). Alanine usage during the LE/PE phase was rather differentiated, as TCA cycle intermediates showed a decrease in ^{13}C-excess compared to than in the E phase, while fatty acids revealed higher ^{13}C-incorporation. In the S phase, utilization of alanine was highest in F-W12 strain. This became especially apparent in lactate (18%), FA (21%), and glutamate (7%) but was also true for glucosamine (3%) as a product of gluconeogenesis.
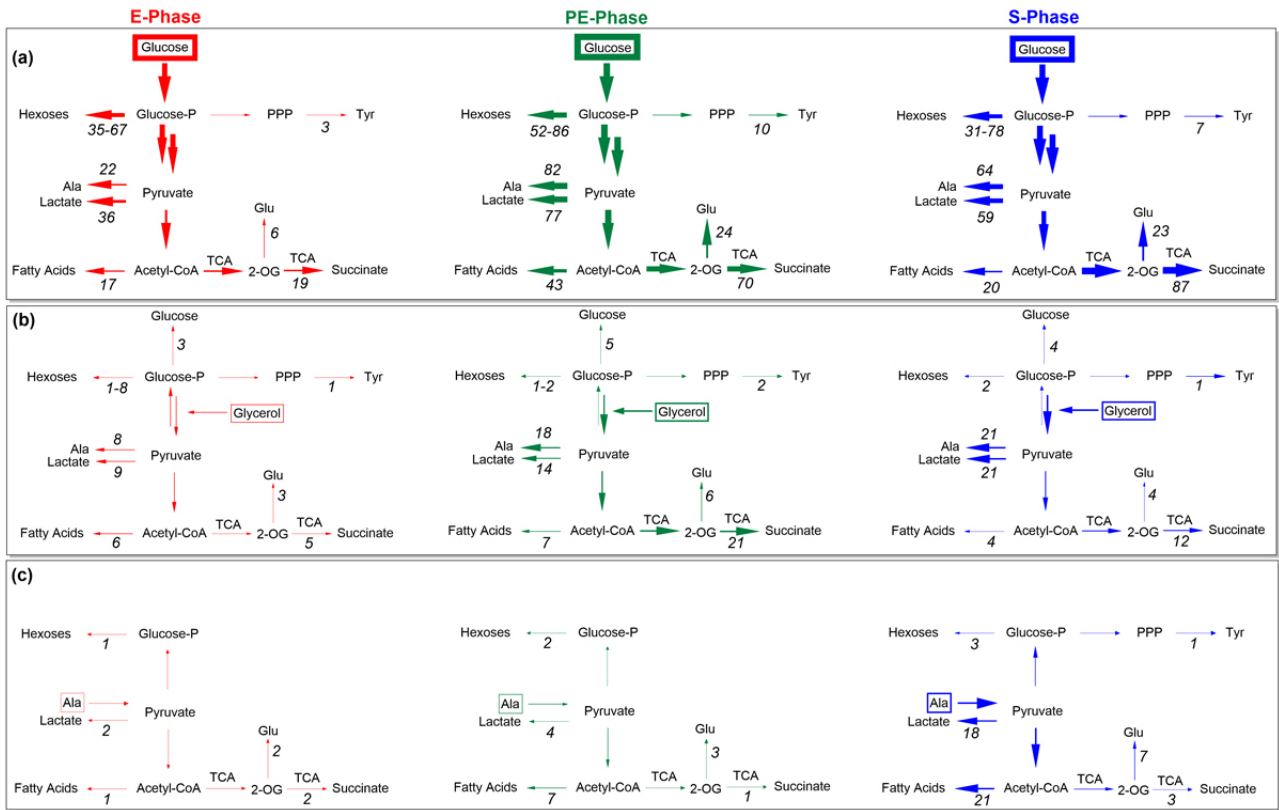
Figure 4: Overview of growth phase-dependent in *Francisella* F-W12 strain. Boxes indicate the supplied ^{13}C-labeled substrates. For more details, see the legend of Figure 2.

Discussion

Glucose as a carbon substrate

Glucose is metabolized in *Francisella* strains mainly via the Embden-Meyerhof-Parnas pathway and via the pentose phosphate pathway (Brissac et al., 2015; Chen et al., 2017; Ziveri et al., 2017b; Rytter et al., 2021). Here, we could confirm that these pathways are highly active during all growth phases, with a glucose usage rate in *Fno*> *Fth*>F-W12. In our comparative study, we could now demonstrate that carbon flux from glucose was highest in the LE/PE phase for all strains under study, underlining the observed positive effect of exogenous glucose on the growth of *Francisella*, especially during the late exponential phase (Figure 1b).

In contrast to *Fth*, the usage of labeled glucose for glucosamine biosynthesis was even still high in the S phase of *Fno* and F-W12. The diverse isotopologue profile in glucosamine clearly reflects that the supplied $^{13}C_6$-glucose (M+6) was directly incorporated into the hexose for, e.g., cell wall biosynthesis (based on the observation of M+6 isotopologues in glucosamine). However, the observation of M+3 isotopologues in glucosamine revealed that exogenous glucose was also first degraded into $^{13}C_3$-trioses followed by glucogenesis where the triple ^{13}C-labeled triose is paired with an unlabeled triose resulting in the detected $^{13}C_3$-hexose specimens.

In relation to the observed differential influence of glucose on the growth of *Fth* in the E phase (Figure 1b) and the reduction of glucose levels in the medium supernatant in the E phase, it seemed that, during exponential growth of *Fth*, more glucose is required for the generation of energy (ATP) through the TCA cycle and respiration as compared to *Fno* and F-W12 that would lead to higher consumption of O_2 and a loss of ^{13}C as $^{13}CO_2$. This could explain why *Fth* incorporated less labeled carbon from glucose than *Fno*, despite apparently consuming more glucose from the medium (Table 1). In addition, due to the absence of glucose-6-phosphate dehydrogenase (ED pathway) and the presence of lactate dehydrogenase (Hill and Mills, 1954; Kanehisa et al., 2016; Radlinski et al., 2018), this may also lead to the observed higher flux into lactate (under O_2 deficit) of *Fth* and thus to a lower carbon flux into metabolites when compared to *Fno* or F-W12. Generally, flux into lactate was high, but only *Fth* showed its maximum already in the E phase.

In addition to early glucose usage through the TCA cycle, it seems that amino acid and protein biosynthesis in *Fth* was highest during the E phase and subsequently reduced in the PE phase as mol% values of labeled protein-bound alanine did not further increase in the PE phase, whereas the ^{13}C-incorporation into free alanine was still high. In contrast, *Fno* and F-W12 showed an increase in the ^{13}C-excess of both free and protein-bound alanine during the PE phase. In comparison to the aquatic F-W12 and *Fno* strains, glucose metabolism seems to play a more relevant role in the apparently more pathogenic *Fth* strain, at least under *in-vitro* conditions, since *Fth* massively used glucose already in the early E phase probably to generate energy via the TCA cycle for, e.g., protein biosynthesis. In

line with this conclusion, glucose also enhanced intracellular growth of *Ftt* in cell culture (Radlinski et al., 2018), and recent studies suggested that intracellular *Francisella* require the pentose phosphate pathway and glycolysis during their initial phase of replication (Rytter et al., 2021).

On the other hand, glycolysis was reported to be dispensable for *Ftt* virulence under *in-vivo* conditions indicating the highly adaptive glucose metabolism of the pathogen. Thus, when intracellular glucose becomes limiting, *Francisella* is capable of switching to gluconeogenesis.

Glycerol as a co-substrate

We here show that *Fth* efficiently takes up glycerol during all growth phases but that it is hardly used as a carbon substrate in the glucose-rich medium T. This stands in contrast to the presence of a glycerol kinase in the *Fth* genome as well as the ability of *Fth* to metabolize glycerol phosphate (Gyuranecz et al., 2010; Huber et al., 2010; Chen et al., 2017), but confirms previous observations regarding the role of glycerol in *Fth* metabolism (Petersen and Schriefer, 2005; Gyuranecz et al., 2010; Huber et al., 2010; Gesbert et al., 2014; Brissac et al., 2015; Chen et al., 2017, 2020). Still, the high uptake rate suggests the utilization of glycerol potentially for the synthesis of glycerolipids which were not analyzed in our study. However, it should be kept in mind that *Ftt* SchuS4 can efficiently metabolize glycerol as a carbon nutrient. Remarkably, this phenotype is used to distinguish *F. tularensis* type A (*Ftt*) from type B (*Fth*) (Petersen and Schriefer, 2005; Gyuranecz et al., 2010; Huber et al., 2010; Mackie et al., 2012). In contrast to *Fth*, glycerol provides a more valuable co-substrate for *Fno* and F-W12 under our conditions, especially during the LE/PE and S phases.

Metabolization mostly occurred via downstream conversion of pyruvate, but there were also indications for gluconeogenesis at low rates. The low gluconeogenetic activity might be due to the high amounts of glucose in the medium, but the labeling data generally proves glycerol's potential as a gluconeogenic substrate. Similar to glucose usage in both strains, glycerol utilization was highest in the LE/PE phase, thereby corroborating the co-usage of these two substrates. Interestingly, in *Fno*, glycerol uptake decreased sharply but remained unchanged in F-W12. Although both strains represent environmental aquatic isolates, there appears to be a difference regarding the role of glycerol during the S phase.

Alanine as a co-substrate

Surprisingly, alanine concentration in medium T during growth increased for all three species under study (Table 1). This may underline the proteolytic activity of *Francisella* strains, leading to the degradation of the available proteins and peptides in the medium (e.g., of brain heart infusion and bacto tryptone). However, in the presence of glucose at high concentrations, alanine may be generated and secreted into the medium in parallel to lactate from pyruvate to regenerate NAD^+,

when O_2 is decreasing, although high amounts of labeled alanine were produced from glucose as a labeled substrate. To confirm this hypothesis, we demonstrated in a control experiment that a high amount of ^{13}C-alanine (27% in the supernatant), generated from ^{13}C-glycerol during the PE/LE phase of growth of *Fno*, was secreted into the medium (Table S28). The data confirm our hypothesis and may also explain the observed increasing amount of alanine within the medium during the growth of the strains investigated (Table 1).

Amino acids are well known to be important for intracellular replicating *Francisella* (Barel et al., 2012; Gesbert et al., 2014; Ramond et al., 2014; Barel et al., 2015; Gesbert et al., 2015; Radlinski et al., 2018). In contrast to glucose or glycerol, we observed that carbon flux from alanine was highest in the S phase into most of the metabolites under study. However, considering the relatively low ^{13}C-incorporation values in comparison to the experiments with labeled glucose or glycerol, it is obvious that alanine and other amino acids are used to a lesser extent as carbon substrates by *Francisella* when growing in medium T, although alanine was reported to be an efficient carbon source in *Fno* (Brissac et al., 2015; Ziveri et al., 2017a).

Specifically, it was observed for *Fno* that the growth reduction by a reduced glucose concentration could be compensated by adding 30 mM alanine (Brissac et al., 2015). We do not know if this is also true for *Fth*, but it is interesting that in the presence of labeled alanine as a co-substrate, nearly no labeled lactate was produced by *Fth*, in contrast to *Fno* and F-W12. In general, carbon flux from alanine was mainly found in fatty acids, lactate, and TCA cycle-related metabolites in the E and S phase. Surprisingly, F-W12 showed the highest alanine usage, especially in the S phase, again underlining the differences between *Fno* and F-W12. The observed low carbon flux rates from labeled amino acids in *Fth* and *Fno* grown in medium T could also be shown for glutamine (preliminary results, data not shown) and may also be due to the high amount of glucose in this medium (Chen et al., 2017).

Conclusion

The specific ^{13}C-patterns in multiple metabolites revealed minor but significant differences in the relative rates of substrate usages and carbon fluxes of the three *Francisella* strains under study. In general, the usage and carbon flux rates into most metabolites was: glucose >> glycerol = alanine. The ^{13}C-isotopologue profiles confirmed that glycerol could serve as a minor gluconeogenic substrate for all studied strains (Chen et al., 2017). This is now demonstrated for the first time also for alanine. Moreover, we here corroborated that the Embden-Meyerhof-Parnas pathway and gluconeogenesis are simultaneously active, as expected before by (Brissac et al., 2015), although glucose was present at high amounts in the medium until the stationary phase.

Glycerol was a good gluconeogenic substrate for *Fno* and F-W12, especially during the early exponential and LE/PE phase. In the LE/PE phase, the carbon flux from glucose and glycerol increased, and the

TCA cycle was more active in all three strains under study. Furthermore, carbon fluxes from glucose or glycerol into lactate increased during the later growth phases. Based on this observation, lactate dehydrogenase (and Glu dehydrogenase) could be important for stabilizing the redox status of the bacteria or for using intracellular lactate as another co-substrate for survival (Radlinski et al., 2018). Regarding the connection between metabolism and virulence, the apparently more virulent *Fth* strain is more dependent on glucose, as its metabolization is initiated earlier compared to *Fno* and F-W12, although the growth of *Fth* was slightly delayed. Also, the overall glucose consumption from the medium was highest for the *Fth* strain, while the potential co-substrates were used to a much lesser extent as compared to *Fno* and F-W12.

Further *in-vivo* studies using different *Fth* WT strains (e.g., different biovars or strains isolated from different hosts) are now necessary to better understand the puzzling role of glucose during the infection cycle of *Fth* as compared to earlier results obtained with *Fno* or *Ftt* (Radlinski et al., 2018; Rytter et al., 2021). However, all data about nutrients usage and metabolism of *Francisella* underline the metabolic plasticity of these bacteria to adjust to environmental conditions rapidly. This might be especially relevant to adapting their metabolism to host cells' rapidly changing milieu during intracellular growth.

References

Appelt, S., Faber, M., Köppen, K., Jacob, D., Grunow, R., Heuner, K., 2020. *Francisella tularensis* subspecies *holarctica* and tularemia in Germany. Microorganisms 8. 10.3390/microorganisms8091448.

Appelt, S., Köppen, K., Radonić, A., Drechsel, O., Jacob, D., Grunow, R., Heuner, K., 2019. Genetic diversity and spatial segregation of *Francisella tularensis* subspecies *holarctica* in Germany. Frontiers in Cellular and Infection Microbiology 9, 376. 10.3389/fcimb.2019.00376.

Barel, M., Meibom, K., Dubail, I., Botella, J., Charbit, A., 2012. *Francisella tularensis* regulates the expression of the amino acid transporter SLC1A5 in infected THP-1 human monocytes. Cellular Microbiology 14, 1769–1783. 10.1111/j.1462-5822.2012.01837.x.

Barel, M., Ramond, E., Gesbert, G., Charbit, A., 2015. The complex amino acid diet of *Francisella* in infected macrophages. Frontiers in Cellular and Infection Microbiology 5, 9. 10.3389/fcimb.2015.00009.

Becker, S., Lochau, P., Jacob, D., Heuner, K., Grunow, R., 2016. Successful re-evaluation of broth medium T for growth of *Francisella tularensis* ssp. and other highly pathogenic bacteria. Journal of Microbiological Methods 121, 5–7. 10.1016/j.mimet.2015.11.018.

Bertani, G., 1951. Studies on lysogenesis. I. the mode of phage liberation by lysogenic *Escherichia coli*. Journal of Bacteriology 62, 293–300. 10.1128/jb.62.3.293-300.1951.

Bertani, G., 2004. Lysogeny at mid-twentieth century: P1, p2, and other experimental systems. Journal of Bacteriology 186, 595–600. 10.1128/JB.186.3.595-600.2004.

Brissac, T., Ziveri, J., Ramond, E., Tros, F., Kock, S., Dupuis, M., Brillet, M., Barel, M., Peyriga, L., Cahoreau, E., Charbit, A., 2015. Gluconeogenesis, an essential metabolic pathway for pathogenic *Francisella*. Molecular Microbiology 98, 518–534. 10.1111/mmi.13139.

Chen, F., Köppen, K., Rydzewski, K., Einenkel, R., Morguet, C., Vu, D.T., Eisenreich, W., Heuner, K., 2020. Myo-inositol as a carbon substrate in *Francisella* and insights into the metabolism of *Francisella* sp. strain w12-1067. International Journal of Medical Microbiology 310, 151426. 10.1016/j.ijmm.2020.151426.

Chen, F., Rydzewski, K., Kutzner, E., Häuslein, I., Schunder, E., Wang, X., Meighen-Berger, K., Grunow, R., Eisenreich, W., Heuner, K., 2017. Differential substrate usage and metabolic fluxes in *Francisella tularensis* subspecies *holarctica* and *Francisella novicida*. Frontiers in Cellular and Infection Microbiology 7, 275. 10.3389/fcimb.2017.00275.

Eisenreich, W., Dandekar, T., Heesemann, J., Goebel, W., 2010. Carbon metabolism of intracellular bacterial pathogens and possible links to virulence. Nature Reviews. Microbiology 8, 401–412. 10.1038/nrmicro2351.

Eisenreich, W., Heesemann, J., Rudel, T., Goebel, W., 2015. Metabolic adaptations of intracellullar bacterial pathogens and their mammalian host cells during infection ("Pathometabolism"). Microbiology Spectrum 3. 10.1128/microbiolspec.MBP-0002-2014.

Ellis, J., Oyston, P.C.F., Green, M., Titball, R.W., 2002. Tularemia. Clinical Microbiology Reviews 15, 631–646. 10.1128/CMR.15.4.631-646.2002.

Gesbert, G., Ramond, E., Rigard, M., Frapy, E., Dupuis, M., Dubail, I., Barel, M., Henry, T., Meibom, K., Charbit, A., 2014. Asparagine assimilation is critical for intracellular replication and dissemination of *Francisella*. Cellular Microbiology 16, 434–449. 10.1111/cmi.12227.

Gesbert, G., Ramond, E., Tros, F., Dairou, J., Frapy, E., Barel, M., Charbit, A., 2015. Importance of branched-chain amino acid utilization in *Francisella* intracellular adaptation. Infection and Immunity 83, 173–183. 10.1128/IAI.02579-14.

Gillmaier, N., Schunder, E., Kutzner, E., Tlapak, H., Rydzewski, K., Herrmann, V., Stämmler, M., Lasch, P., Eisenreich, W., Heuner, K., 2016. Growth-related metabolism of the carbon storage poly-3-hydroxybutyrate in *Legionella pneumophila*. Journal of Biolgical Chemistry 291, 6471–82. 10.1074/jbc.M115.693481.

Grubmüller, S., Schauer, K., Goebel, W., Fuchs, T.M., Eisenreich, W., 2014. Analysis of carbon substrates used by *Listeria monocytogenes* during growth in J774A.1 macrophages suggests a bipartite intracellular metabolism. Frontiers in Cellular and Infection Microbiology 4, 156. 10.3389/fcimb.2014.00156.

Gyuranecz, M., Erdélyi, K., Fodor, L., Jánosi, K., Szépe, B., Füleki, M., Szoke, I., Dénes, B., Makrai, L., 2010. Characterization of *Francisella tularensis* strains, comparing their carbon source utilization. Zoonoses and Public Health 57, 417–422. 10.1111/j.1863-2378.2009.01238.x.

Hill, R.L., Mills, R.C., 1954. The anaerobic glucose metabolism of *Bacterium tularense*. Archives of Biochemistry and Biophysics 53, 174–183. 10.1016/0003-9861(54)90244-1.

Huber, B., Escudero, R., Busse, H.J., Seibold, E., Scholz, H.C., Anda, P., Kämpfer, P., Splettstoesser, W.D., 2010. Description of *Francisella hispaniensis* sp. *nov.*, isolated from human blood, reclassification of *Francisella novicida* (larson et al. 1955) olsufiev et al. 1959 as *Francisella tularensis* subsp. *novicida* comb. *nov.* and emended description of the genus *Francisella*. International Journal of Systematic and Evolutionary Microbiology 60, 1887–1896. 10.1099/ijs.0.015941-0.

Kanehisa, M., Sato, Y., Kawashima, M., Furumichi, M., Tanabe, M., 2016. KEGG as a reference resource for gene and protein annotation. Nucleic Acids Research 44, D457–62. 10.1093/nar/gkv1070.

Köppen, K., Chen, F., Rydzewski, K., Einenkel, R., Böttcher, T., Morguet, C., Grunow, R., Eisenreich, W., Heuner, K., 2019. Screen for fitness and virulence factors of *Francisella* sp. strain w12-1067 using amoebae. International Journal of Medical Microbiology 309, 151341. 10.1016/j.ijmm.2019.151341.

Larson, C.F., Wicht, W., Jellison, W.F., 1955. A new organism resembling *P. tularensis* isolated from water. Publich Health Reports 70, 253–258. URL: https://pubmed.ncbi.nlm.nih.gov/14357545/.

Mackie, R.S., McKenney, E.S., van Hoek, M.L., 2012. Resistance of *Francisella novicida* to fosmidomycin associated with mutations in the glycerol-3-phosphate transporter. Frontiers in Microbiology 3, 226. `10.3389/fmicb.2012.00226`.

Petersen, J.M., Schriefer, M.E., 2005. Tularemia: emergence/re-emergence. Veterinary Research 36, 455–467. `10.1051/vetres:2005006`.

Radlinski, L.C., Brunton, J., Steele, S., Taft-Benz, S., Kawula, T.H., 2018. Defining the metabolic pathways and host-derived carbon substrates required for *Francisella tularensis* intracellular growth. mBio 9. `10.1128/mBio.01471-18`.

Ramond, E., Gesbert, G., Rigard, M., Dairou, J., Dupuis, M., Dubail, I., Meibom, K., Henry, T., Barel, M., Charbit, A., 2014. Glutamate utilization couples oxidative stress defense and the tricarboxylic acid cycle in *Francisella* phagosomal escape. PLoS Pathogens 10, e1003893. `10.1371/journal.ppat.1003893`.

Rydzewski, K., Schulz, T., Brzuszkiewicz, E., Holland, G., Lück, C., Fleischer, J., Grunow, R., Heuner, K., 2014. Genome sequence and phenotypic analysis of a first german *Francisella* sp. isolate (w12-1067) not belonging to the species *Francisella tularensis*. BMC Microbiology 14, 169. `10.1186/1471-2180-14-169`.

Rytter, H., Jamet, A., Ziveri, J., Ramond, E., Coureuil, M., Lagouge-Roussey, P., Euphrasie, D., Tros, F., Goudin, N., Chhuon, C., Nemazanyy, I., de Moraes, F.E., Labate, C., Guerrera, I.C., Charbit, A., 2021. The pentose phosphate pathway constitutes a major metabolic hub in pathogenic *Francisella*. PLoS Pathogens 17, e1009326. `10.1371/journal.ppat.1009326`.

Schulze, C., Heuner, K., Myrtennäs, K., Karlsson, E., Jacob, D., Kutzer, P., Große, K., Forsman, M., Grunow, R., 2016. High and novel genetic diversity of *Francisella tularensis* in germany and indication of environmental persistence. Epidemiology and Infection 144, 3025–3036. `10.1017/S0950268816001175`.

Siddaramappa, S., Challacombe, J.F., Petersen, J.M., Pillai, S., Hogg, G., Kuske, C.R., 2011. Common ancestry and novel genetic traits of *Francisella novicida*-like isolates from North America and Australia as revealed by comparative genomic analyses. Applied and Environmental Microbiology 77, 5110–5122. `10.1128/AEM.00337-11`.

Sjöstedt, A., 2011. Special topic on *Francisella tularensis* and tularemia. Frontiers in Microbiology 2, 86. `10.3389/fmicb.2011.00086`.

Sundell, D., Uneklint, I., Öhrman, C., Salomonsson, E., Karlsson, L., Bäckman, S., Näslund, J., Sjödin, A., Forsman, M., Appelt, S., Drechsel, O., Jacob, D., Heuner, K., Myrtennäs, K., 2020. Complete genome sequence of *Francisella tularensis* subsp. *holarctica* strain a271_1 (FDC408), isolated from a Eurasian Beaver (Castor fiber). Microbiology Resource Announcements 9. `10.1128/MRA.00738-20`.

Ziveri, J., Barel, M., Charbit, A., 2017a. Importance of metabolic adaptations in *Francisella* pathogenesis. Frontiers in Cellular and Infection Microbiology 7, 96. `10.3389/fcimb.2017.00096`.

Ziveri, J., Tros, F., Guerrera, I.C., Chhuon, C., Audry, M., Dupuis, M., Barel, M., Korniotis, S., Fillatreau, S., Gales, L., Cahoreau, E., Charbit, A., 2017b. The metabolic enzyme fructose-1,6-bisphosphate aldolase acts as a transcriptional regulator in pathogenic *Francisella*. Nature Communications 8, 853. `10.1038/s41467-017-00889-7`.

Table S1: ^{13}C-Excess of proteinogenic amino acids in *Fth*, *Fno* and F-W12 during the exponential growth phase in medium T with the addition of 11 mM [U-^{13}C$_6$]glucose. Mean values and standard deviations are based on two biological replicates with three technical replicates each.

	Fth		Fno		F. W12	
	Mean	SD	Mean	SD	Mean	SD
Ala	5,26%	0,26%	6,16%	1,19%	1,50%	0,19%
Asp	1,01%	0,06%	0,32%	0,13%	0,20%	0,08%
Glu	2,00%	0,08%	2,96%	0,56%	0,74%	0,07%
Gly	0,27%	0,05%	0,23%	0,08%	0,18%	0,05%
His	0,21%	0,03%	0,05%	0,04%	0,40%	0,36%
Ile	0,15%	0,03%	0,11%	0,06%	0,10%	0,03%
Leu	0,18%	0,03%	0,05%	0,05%	0,05%	0,04%
Lys	0,26%	0,03%	0,07%	0,02%	0,08%	0,01%
Met	0,11%	0,04%	0,07%	0,10%	0,07%	0,04%
Phe	0,28%	0,04%	0,10%	0,03%	0,24%	0,02%
Pro	0,51%	0,09%	0,29%	0,02%	0,25%	0,03%
Ser	0,89%	0,09%	0,16%	0,02%	0,13%	0,03%
Thr	0,78%	0,05%	0,40%	0,08%	0,40%	0,10%
Tyr	1,45%	0,41%	1,49%	0,19%	0,38%	0,07%
Val	0,09%	0,01%	0,05%	0,03%	0,01%	0,01%

Table S2: ^{13}C-Excess of proteinogenic amino acids in *Fth*, *Fno* and F-W12 during the post exponential/late exponential growth phase in medium T with the addition of 11 mM [U-^{13}C$_6$]glucose. Mean values and standard deviations are based on two biological replicates with three technical replicates each.

	Fth		Fno		F. W12	
	Mean	SD	Mean	SD	Mean	SD
Ala	6,95%	0,73%	7,25%	0,30%	4,79%	0,44%
Asp	2,23%	0,45%	0,61%	0,13%	0,85%	0,14%
Glu	4,04%	0,39%	3,49%	0,27%	1,96%	0,04%
Gly	0,26%	0,04%	0,75%	0,10%	0,38%	0,05%
His	0,21%	0,03%	0,02%	0,02%	0,05%	0,03%
Ile	0,14%	0,02%	0,09%	0,03%	0,13%	0,04%
Leu	0,15%	0,04%	0,07%	0,03%	0,07%	0,05%
Lys	0,23%	0,03%	0,09%	0,01%	0,09%	0,02%
Met	0,12%	0,07%	0,11%	0,09%	0,14%	0,11%
Phe	0,20%	0,05%	0,16%	0,06%	0,13%	0,04%
Pro	0,47%	0,08%	0,26%	0,07%	0,27%	0,02%
Ser	0,85%	0,07%	0,49%	0,06%	2,26%	0,09%
Thr	0,75%	0,07%	0,52%	0,08%	0,46%	0,07%
Tyr	1,67%	0,37%	1,41%	0,11%	0,94%	0,05%
Val	0,09%	0,02%	0,08%	0,04%	0,01%	0,01%

Table S3: ^{13}C-Excess of proteinogenic amino acids in *Fth*, *Fno* and F-W12 during the stationary growth phase in medium T with the addition of 11 mM [U-^{13}C$_6$]glucose. Mean values and standard deviations are based on two biological replicates with three technical replicates each.

	Fth		*Fno*		*F. W12*	
	Mean	SD	Mean	SD	Mean	SD
Ala	5,28%	0,02%	6,58%	0,36%	3,76%	0,43%
Asp	1,43%	0,15%	1,05%	0,12%	0,60%	0,15%
Glu	2,60%	0,13%	3,31%	0,14%	1,62%	0,15%
Gly	0,26%	0,04%	1,37%	0,13%	0,21%	0,07%
His	0,20%	0,03%	0,04%	0,02%	0,05%	0,02%
Ile	0,13%	0,03%	0,12%	0,04%	0,09%	0,05%
Leu	0,16%	0,03%	0,09%	0,06%	0,07%	0,04%
Lys	0,26%	0,04%	0,08%	0,03%	0,08%	0,01%
Met	0,13%	0,03%	0,23%	0,23%	0,07%	0,05%
Phe	0,16%	0,01%	0,22%	0,07%	0,23%	0,07%
Pro	0,49%	0,07%	0,26%	0,04%	0,27%	0,03%
Ser	0,88%	0,08%	1,35%	0,08%	1,65%	0,22%
Thr	0,74%	0,05%	0,46%	0,06%	0,44%	0,06%
Tyr	1,18%	0,38%	2,33%	0,09%	0,93%	0,10%
Val	0,09%	0,04%	0,01%	0,01%	0,01%	0,01%

Table S4: ^{13}C-Excess of proteinogenic amino acids in *Fth*, *Fno* and F-W12 during the exponential growth phase in medium T with the addition of 25 mM [U-^{13}C$_3$]glycerol. Mean values and standard deviations are based on two biological replicates with three technical replicates each.

	Fth		*Fno*		*F. W12*	
	Mean	SD	Mean	SD	Mean	SD
Ala	2,46%	0,05%	16,13%	0,32%	6,46%	0,19%
Asp	0,60%	0,07%	0,68%	0,24%	0,16%	0,10%
Glu	1,12%	0,13%	8,85%	0,18%	2,25%	0,08%
Gly	0,19%	0,04%	0,54%	0,05%	0,12%	0,05%
His	0,21%	0,03%	1,22%	1,53%	0,13%	0,10%
Ile	0,13%	0,04%	0,14%	0,03%	0,09%	0,02%
Leu	0,14%	0,03%	0,05%	0,06%	0,03%	0,03%
Lys	0,23%	0,04%	0,10%	0,04%	0,09%	0,02%
Met	0,64%	0,78%	0,19%	0,20%	1,12%	0,09%
Phe	0,17%	0,02%	0,14%	0,01%	0,82%	0,08%
Pro	0,48%	0,08%	0,23%	0,08%	0,23%	0,04%
Ser	0,81%	0,06%	0,28%	0,06%	0,19%	0,11%
Thr	0,73%	0,06%	0,38%	0,13%	0,28%	0,13%
Tyr	1,11%	0,51%	3,43%	0,15%	1,37%	0,20%
Val	0,06%	0,02%	0,16%	0,01%	0,02%	0,02%

Table S5: ^{13}C-Excess of proteinogenic amino acids in *Fth*, *Fno* and F-W12 during the post exponential/late exponential growth phase in medium T with the addition of 25 mM [U-[13]C$_3$]glycerol. Mean values and standard deviations are based on two biological replicates with three technical replicates each.

	Fth		*Fno*		*F. W12*	
	Mean	SD	Mean	SD	Mean	SD
Ala	1,43%	0,15%	19,39%	0,28%	12,17%	0,68%
Asp	0,56%	0,10%	1,30%	0,14%	0,78%	0,08%
Glu	0,98%	0,13%	9,19%	0,12%	4,05%	0,37%
Gly	0,18%	0,03%	1,83%	0,04%	0,33%	0,12%
His	0,16%	0,04%	0,09%	0,07%	0,28%	0,35%
Ile	0,12%	0,03%	0,13%	0,04%	0,05%	0,03%
Leu	0,12%	0,03%	0,07%	0,03%	0,03%	0,02%
Lys	0,20%	0,04%	0,09%	0,03%	0,08%	0,04%
Met	1,86%	1,67%	0,18%	0,16%	1,52%	2,54%
Phe	0,11%	0,01%	0,14%	0,07%	0,20%	0,10%
Pro	0,43%	0,09%	0,34%	0,09%	0,23%	0,04%
Ser	0,79%	0,06%	1,71%	0,33%	4,04%	0,48%
Thr	0,66%	0,07%	0,51%	0,06%	0,32%	0,14%
Tyr	1,58%	0,59%	2,86%	0,08%	1,57%	0,08%
Val	0,07%	0,02%	0,16%	0,03%	0,01%	0,02%

Table S6: ^{13}C-Excess of proteinogenic amino acids in *Fth*, *Fno* and F-W12 during the stationary growth phase in medium T with the addition of 25 mM [U-[13]C$_3$]glycerol. Mean values and standard deviations are based on two biological replicates with three technical replicates each.

	Fth		*Fno*		*F. W12*	
	Mean	SD	Mean	SD	Mean	SD
Ala	0,18%	0,02%	8,31%	0,64%	12,53%	5,35%
Asp	0,44%	0,09%	0,67%	0,54%	0,21%	0,22%
Glu	0,30%	0,10%	2,68%	0,87%	2,02%	0,21%
Gly	0,18%	0,04%	0,91%	0,42%	0,11%	0,07%
His	0,16%	0,03%	0,06%	0,04%	0,03%	0,03%
Ile	0,13%	0,02%	0,10%	0,05%	0,08%	0,05%
Leu	0,11%	0,02%	0,07%	0,06%	0,06%	0,07%
Lys	0,21%	0,04%	0,08%	0,03%	0,15%	0,22%
Met	2,15%	1,12%	0,22%	0,25%	0,23%	0,46%
Phe	0,07%	0,01%	0,21%	0,08%	0,42%	0,37%
Pro	0,47%	0,06%	0,30%	0,08%	0,28%	0,12%
Ser	0,86%	0,08%	1,01%	0,48%	1,33%	0,83%
Thr	0,66%	0,05%	0,43%	0,06%	0,79%	0,65%
Tyr	1,48%	0,39%	1,64%	0,36%	1,05%	0,40%
Val	0,05%	0,03%	0,04%	0,04%	0,03%	0,03%

Table S7: ^{13}C-Excess of proteinogenic amino acids in *Fth*, *Fno* and F-W12 during the exponential growth phase in medium T with the addition of 5 mM [2,3-[13]C$_2$]alanine. Mean values and standard deviations are based on two biological replicates with three technical replicates each.

	Fth		*Fno*		*F. W12*	
	Mean	SD	Mean	SD	Mean	SD
Ala	5,38%	0,16%	9,57%	1,18%	12,16%	0,21%
Asp	1,33%	0,09%	0,66%	0,20%	0,49%	0,28%
Glu	2,11%	0,16%	3,27%	0,20%	1,83%	0,58%
Gly	0,13%	0,09%	0,21%	0,08%	0,13%	0,16%
Ile	0,17%	0,04%	0,10%	0,04%	0,09%	0,03%
Leu	0,24%	0,07%	0,08%	0,09%	0,10%	0,09%
Lys	0,30%	0,09%	0,20%	0,12%	0,23%	0,12%
Pro	0,42%	0,02%	0,42%	0,11%	0,38%	0,20%
Ser	0,95%	0,08%	0,95%	0,21%	0,88%	0,13%
Thr	0,60%	0,06%	0,48%	0,09%	0,54%	0,22%
Tyr	0,20%	0,03%	0,17%	0,09%	0,18%	0,04%
Val	0,19%	0,06%	0,14%	0,05%	0,05%	0,06%

Table S8: ^{13}C-Excess of proteinogenic amino acids in *Fth*, *Fno* and F-W12 during the post exponential/late exponential growth phase in medium T with the addition of 5 mM [2,3-[13]C$_2$]alanine. Mean values and standard deviations are based on two biological replicates with three technical replicates each.

	Fth		*Fno*		*F. W12*	
	Mean	SD	Mean	SD	Mean	SD
Ala	3,37%	0,32%	3,04%	0,33%	6,52%	0,35%
Asp	1,78%	0,69%	0,60%	0,16%	0,87%	0,17%
Glu	2,71%	0,43%	1,30%	0,11%	2,11%	0,44%
Gly	0,22%	0,31%	0,17%	0,08%	0,16%	0,08%
Ile	0,25%	0,07%	0,16%	0,06%	0,17%	0,09%
Leu	0,24%	0,09%	0,16%	0,05%	0,28%	0,12%
Lys	0,24%	0,22%	0,19%	0,20%	0,21%	0,15%
Pro	0,40%	0,32%	0,53%	0,28%	0,52%	0,33%
Ser	0,93%	0,24%	0,81%	0,07%	0,89%	0,11%
Thr	0,79%	0,21%	0,57%	0,06%	0,54%	0,12%
Tyr	0,22%	0,16%	0,18%	0,13%	0,14%	0,06%
Val	0,11%	0,08%	0,14%	0,07%	0,07%	0,04%

Table S9: ^{13}C-Excess of proteinogenic amino acids in *Fth*, *Fno* and F-W12 during the stationary growth phase in medium T with the addition of 5 mM [2,3-$^{13}C_2$]alanine. Mean values and standard deviations are based on two biological replicates with three technical replicates each.

	Fth		*Fno*		*F. W12*	
	Mean	SD	Mean	SD	Mean	SD
Ala	1,43%	0,56%	1,29%	0,21%	2,13%	0,55%
Asp	0,61%	0,43%	0,49%	0,13%	0,52%	0,33%
Glu	0,99%	1,02%	0,61%	0,16%	0,91%	0,21%
Gly	0,30%	0,29%	0,06%	0,12%	0,19%	0,14%
Ile	0,20%	0,07%	0,12%	0,08%	0,17%	0,05%
Leu	0,09%	0,07%	0,08%	0,07%	0,13%	0,09%
Lys	0,13%	0,09%	0,17%	0,12%	0,24%	0,13%
Pro	0,71%	0,06%	0,40%	0,07%	0,47%	0,29%
Ser	0,75%	0,12%	0,90%	0,17%	0,90%	0,17%
Thr	0,47%	0,12%	0,58%	0,16%	0,53%	0,24%
Tyr	0,13%	0,04%	0,11%	0,05%	0,20%	0,04%
Val	0,08%	0,04%	0,09%	0,07%	0,06%	0,10%

Table S10: ^{13}C-Excess of cytosolic metabolites in *Fth*, *Fno* and F-W12 during the exponential growth phase in medium T with the addition of 11 mM [U-$^{13}C_6$]glucose. Mean values and standard deviations are based on two biological replicates with three technical replicates each.

	Fth		*Fno*		*F. W12*	
	Mean	SD	Mean	SD	Mean	SD
Ala	8,16%	0,48%	8,46%	1,97%	2,75%	0,32%
Asp	0,71%	0,07%	0,12%	0,06%	0,05%	0,07%
Gly	0,20%	0,04%	0,15%	0,07%	0,04%	0,04%
Glu	3,23%	0,27%	3,66%	0,79%	0,76%	0,22%
Ile	0,57%	0,07%	0,29%	0,16%	0,28%	0,10%
Leu	0,19%	0,02%	0,03%	0,04%	0,02%	0,02%
Ser	1,18%	0,08%	0,82%	0,41%	0,96%	0,32%
Thr	0,06%	0,05%	0,12%	0,08%	0,13%	0,08%
Val	0,09%	0,01%	0,04%	0,02%	0,01%	0,01%
Fumarate	2,08%	0,45%	3,92%	1,26%	1,31%	0,48%
Glycerol	8,42%	0,41%	10,12%	2,43%	5,36%	0,44%
Lactate	5,28%	0,29%	8,56%	2,10%	4,61%	0,61%
Palmitate	3,09%	0,19%	4,73%	1,21%	1,44%	0,16%
Stearate	4,48%	0,28%	5,39%	1,40%	2,12%	0,23%
Succinate	1,64%	0,33%	4,19%	1,02%	2,44%	1,35%
Fructose	10,87%	0,91%	11,74%	2,62%	8,58%	4,37%

Table S11: ^{13}C-Excess of cytosolic metabolites in *Fth*, *Fno* and F-W12 during the post exponential/late exponential growth phase in medium T with the addition of 11 mM [U-[13]C$_6$]glucose. Mean values and standard deviations are based on two biological replicates with three technical replicates each.

	Fth		Fno		F. W12	
	Mean	SD	Mean	SD	Mean	SD
Ala	12,39%	0,56%	10,07%	1,04%	8,01%	0,23%
Asp	0,55%	0,06%	0,52%	0,19%	0,18%	0,12%
Gly	0,25%	0,04%	0,69%	0,15%	0,32%	0,09%
Glu	3,25%	0,13%	4,89%	0,52%	2,38%	0,33%
Ile	0,56%	0,06%	0,35%	0,09%	0,22%	0,11%
Leu	0,18%	0,02%	0,02%	0,02%	0,04%	0,03%
Ser	1,24%	0,07%	0,78%	0,46%	0,70%	0,24%
Thr	0,10%	0,06%	0,17%	0,11%	0,12%	0,09%
Val	0,08%	0,02%	0,03%	0,03%	0,01%	0,02%
Fumarate	3,64%	0,19%	4,85%	1,45%	1,94%	0,86%
Glycerol	9,58%	0,09%	9,72%	0,44%	5,25%	1,26%
Lactate	5,87%	0,44%	9,03%	0,65%	7,56%	0,40%
Palmitate	4,10%	0,11%	5,19%	0,22%	3,57%	0,23%
Stearate	6,36%	0,34%	6,98%	0,22%	4,22%	0,40%
Succinate	5,38%	0,19%	5,89%	0,87%	6,88%	4,13%
Fructose	9,54%	0,72%	9,50%	3,70%	8,42%	4,93%

Table S12: ^{13}C-Excess of cytosolic metabolites in *Fth*, *Fno* and F-W12 during the stationary growth phase in medium T with the addition of 11 mM [U-[13]C$_6$]glucose. Mean values and standard deviations are based on two biological replicates with three technical replicates each.

	Fth		Fno		F. W12	
	Mean	SD	Mean	SD	Mean	SD
Ala	14,11%	0,15%	13,43%	2,23%	8,84%	0,49%
Asp	0,55%	0,05%	0,43%	0,27%	0,30%	0,28%
Gly	0,17%	0,05%	2,25%	0,25%	0,06%	0,04%
Glu	2,37%	0,36%	6,11%	0,30%	3,25%	0,11%
Ile	0,55%	0,06%	0,26%	0,10%	0,28%	0,12%
Leu	0,16%	0,02%	0,02%	0,02%	0,03%	0,02%
Ser	1,24%	0,10%	1,01%	0,33%	0,50%	0,15%
Thr	0,08%	0,06%	0,21%	0,08%	0,13%	0,03%
Val	0,07%	0,02%	0,06%	0,03%	0,02%	0,03%
Fumarate	3,56%	0,63%	8,33%	1,40%	2,48%	1,02%
Glycerol	10,00%	0,55%	12,85%	1,13%	4,80%	0,41%
Lactate	3,70%	1,28%	13,32%	1,45%	8,21%	0,70%
Palmitate	3,35%	0,39%	5,26%	0,11%	2,30%	0,26%
Stearate	5,64%	0,35%	7,37%	0,09%	2,84%	0,36%
Succinate	4,85%	0,08%	11,88%	2,64%	12,17%	14,12%
Fructose	8,59%	1,07%	7,89%	3,61%	10,79%	4,77%

Table S13: ^{13}C-Excess of cytosolic metabolites in *Fth*, *Fno* and F-W12 during the exponential growth phase in medium T with the addition of 25 mM [U-[13]C$_3$]glycerol. Mean values and standard deviations are based on two biological replicates with three technical replicates each.

	Fth		Fno		F. W12	
	Mean	SD	Mean	SD	Mean	SD
Ala	3,54%	0,06%	12,44%	0,34%	8,22%	0,25%
Asp	0,56%	0,07%	0,21%	0,14%	0,08%	0,10%
Gly	0,12%	0,04%	0,43%	0,16%	0,09%	0,08%
Glu	2,00%	0,35%	9,65%	0,13%	2,46%	0,17%
Ile	0,58%	0,06%	0,03%	0,03%	0,34%	0,09%
Leu	0,18%	0,02%	0,28%	0,04%	0,02%	0,04%
Ser	1,23%	0,09%	1,11%	0,44%	0,47%	0,24%
Thr	0,05%	0,03%	0,15%	0,13%	0,06%	0,08%
Val	0,08%	0,02%	0,12%	0,05%	0,01%	0,01%
Fumarate	0,55%	0,02%	10,93%	2,41%	3,00%	1,25%
Glycerol	87,22%	0,03%	87,72%	0,33%	92,49%	1,08%
Lactate	0,77%	0,05%	10,96%	0,45%	9,16%	0,24%
Palmitate	1,48%	0,07%	9,69%	4,39%	3,81%	2,31%
Stearate	2,62%	0,08%	11,09%	3,13%	5,82%	1,87%
Succinate	1,14%	0,09%	11,84%	1,82%	4,79%	3,01%
Fructose	0,83%	0,13%	2,82%	0,83%	1,38%	1,37%

Table S14: ^{13}C-Excess of cytosolic metabolites in *Fth*, *Fno* and F-W12 during the post exponential/late exponential growth phase in medium T with the addition of 25 mM [U-[13]C$_3$]glycerol. Mean values and standard deviations are based on two biological replicates with three technical replicates each.

	Fth		Fno		F. W12	
	Mean	SD	Mean	SD	Mean	SD
Ala	2,39%	0,28%	23,68%	0,90%	18,09%	1,42%
Asp	0,42%	0,03%	0,29%	0,25%	0,39%	0,24%
Gly	0,12%	0,02%	2,28%	0,12%	0,63%	0,09%
Glu	1,13%	0,34%	15,00%	0,45%	6,38%	0,77%
Ile	0,58%	0,06%	0,03%	0,03%	0,27%	0,12%
Leu	0,16%	0,02%	0,31%	0,09%	0,01%	0,01%
Ser	1,19%	0,12%	0,93%	0,29%	0,94%	0,33%
Thr	0,06%	0,07%	0,20%	0,11%	0,16%	0,10%
Val	0,11%	0,03%	0,12%	0,02%	0,02%	0,03%
Fumarate	0,36%	0,11%	14,54%	1,28%	5,14%	1,54%
Glycerol	85,52%	1,77%	80,67%	0,86%	95,14%	3,29%
Lactate	0,69%	0,05%	16,98%	0,41%	14,31%	0,92%
Palmitate	0,95%	0,10%	9,95%	4,45%	5,16%	2,59%
Stearate	1,81%	0,18%	14,45%	3,94%	6,87%	2,39%
Succinate	0,42%	0,11%	21,52%	1,53%	20,58%	17,32%
Fructose	0,90%	0,40%	1,32%	0,35%	0,81%	0,28%

Table S15: ^{13}C-Excess of cytosolic metabolites in *Fth*, *Fno* and F-W12 during the stationary growth phase in medium T with the addition of 25 mM [U-^{13}C$_3$]glycerol. Mean values and standard deviations are based on two biological replicates with three technical replicates each.

	Fth		*Fno*		*F. W12*	
	Mean	SD	Mean	SD	Mean	SD
Ala	0,15%	0,02%	18,53%	1,67%	20,81%	1,81%
Asp	0,36%	0,02%	0,09%	0,17%	0,02%	0,04%
Gly	0,01%	0,02%	1,29%	0,47%	0,09%	0,11%
Glu	0,25%	0,02%	4,27%	0,32%	3,70%	1,21%
Ile	0,58%	0,07%	0,06%	0,06%	0,28%	0,13%
Leu	0,20%	0,03%	0,36%	0,11%	0,05%	0,03%
Ser	1,25%	0,10%	0,74%	0,34%	0,73%	0,15%
Thr	0,07%	0,04%	0,12%	0,09%	0,16%	0,16%
Val	0,09%	0,02%	0,12%	0,04%	0,01%	0,01%
Fumarate	0,11%	0,05%	12,87%	5,49%	2,50%	1,12%
Glycerol	85,23%	1,07%	49,01%	26,43%	96,95%	1,48%
Lactate	0,30%	0,03%	13,42%	1,89%	20,89%	1,03%
Palmitate	0,19%	0,06%	5,09%	3,81%	2,47%	1,72%
Stearate	0,52%	0,14%	10,09%	4,28%	4,10%	2,54%
Succinate	0,09%	0,01%	18,73%	0,81%	11,94%	1,06%
Fructose	0,81%	0,67%	1,28%	0,55%	2,02%	1,55%

Table S16: ^{13}C-Excess of cytosolic metabolites in *Fth*, *Fno* and F-W12 during the exponential growth phase in medium T with the addition of 5 mM [2,3-^{13}C$_2$]alanine. Mean values and standard deviations are based on two biological replicates with three technical replicates each.

	Fth		*Fno*		*F. W12*	
	Mean	SD	Mean	SD	Mean	SD
Ala	7,12%	0,34%	8,53%	0,42%	4,90%	0,39%
Asp	0,68%	0,08%	0,39%	0,14%	0,58%	0,31%
Gly	0,17%	0,05%	0,14%	0,08%	0,13%	0,18%
Glu	2,78%	0,15%	2,92%	0,22%	1,88%	0,53%
Ile	0,55%	0,08%	0,45%	0,05%	0,46%	0,07%
Leu	0,09%	0,06%	0,10%	0,08%	0,11%	0,11%
Ser	1,25%	0,22%	1,41%	0,29%	1,42%	0,20%
Thr	0,14%	0,07%	0,20%	0,05%	0,18%	0,11%
Val	0,11%	0,08%	0,04%	0,02%	0,12%	0,12%
Fumarate	1,18%	0,25%	3,28%	0,56%	1,53%	1,52%
Glycerol	1,06%	0,14%	0,81%	0,24%	1,05%	0,24%
Lactate	0,29%	0,15%	4,01%	0,17%	1,68%	0,16%
Palmitate	3,08%	0,20%	5,75%	0,55%	0,84%	0,40%
Stearate	2,03%	0,12%	3,81%	0,67%	0,75%	0,33%
Succinate	0,99%	0,09%	2,18%	0,30%	2,20%	0,67%
Fructose	0,94%	0,36%	1,48%	0,91%	0,91%	0,15%

Table S17: ^{13}C-Excess of cytosolic metabolites in *Fth*, *Fno* and F-W12 during the post exponential/late exponential growth phase in medium T with the addition of 5 mM [2,3-^{13}C$_2$]alanine. Mean values and standard deviations are based on two biological replicates with three technical replicates each.

	Fth		*Fno*		*F. W12*	
	Mean	SD	Mean	SD	Mean	SD
Ala	2,92%	0,09%	6,55%	0,72%	5,14%	0,39%
Asp	0,38%	0,10%	0,42%	0,14%	0,41%	0,15%
Gly	0,10%	0,12%	0,12%	0,09%	0,02%	0,03%
Glu	1,62%	0,57%	1,43%	0,35%	1,64%	0,11%
Ile	0,46%	0,07%	0,42%	0,11%	0,51%	0,10%
Leu	0,09%	0,03%	0,07%	0,04%	0,10%	0,06%
Ser	1,15%	0,30%	1,25%	0,25%	1,13%	0,21%
Thr	0,19%	0,16%	0,27%	0,17%	0,25%	0,13%
Val	0,07%	0,03%	0,06%	0,06%	0,07%	0,04%
Fumarate	0,87%	0,41%	1,46%	0,84%	0,88%	0,48%
Glycerol	0,71%	0,23%	0,79%	0,15%	0,80%	0,35%
Lactate	0,21%	0,03%	4,04%	0,76%	2,46%	0,27%
Palmitate	2,77%	0,50%	1,79%	0,46%	3,78%	1,37%
Stearate	2,09%	0,61%	2,32%	0,73%	4,35%	0,99%
Succinate	0,98%	0,17%	0,65%	0,07%	0,42%	0,24%
Fructose	0,91%	0,23%	0,79%	0,22%	1,04%	0,41%

Table S18: ^{13}C-Excess of cytosolic metabolites in *Fth*, *Fno* and F-W12 during the stationary growth phase in medium T with the addition of 5 mM [2,3-^{13}C$_2$]alanine. Mean values and standard deviations are based on two biological replicates with three technical replicates each.

	Fth		*Fno*		*F. W12*	
	Mean	SD	Mean	SD	Mean	SD
Ala	4,76%	2,73%	6,32%	0,15%	12,40%	1,38%
Asp	0,29%	0,09%	0,58%	0,21%	0,54%	0,19%
Gly	0,10%	0,11%	0,07%	0,10%	0,10%	0,12%
Glu	0,75%	0,22%	1,10%	0,66%	2,11%	0,18%
Ile	0,42%	0,09%	0,40%	0,10%	0,47%	0,06%
Leu	0,10%	0,06%	0,22%	0,24%	0,10%	0,08%
Ser	1,37%	0,32%	1,51%	0,32%	1,30%	0,10%
Thr	0,30%	0,11%	0,31%	0,16%	0,26%	0,12%
Val	0,08%	0,06%	0,06%	0,04%	0,06%	0,05%
Fumarate	0,50%	0,14%	2,24%	0,89%	2,02%	0,39%
Glycerol	0,84%	0,08%	0,82%	0,29%	0,89%	0,10%
Lactate	0,15%	0,04%	3,87%	0,29%	5,41%	0,26%
Palmitate	0,88%	0,58%	0,88%	0,70%	5,08%	0,30%
Stearate	1,33%	0,33%	1,23%	0,50%	6,29%	0,69%
Succinate	0,44%	0,13%	1,20%	0,17%	0,86%	0,60%
Fructose	0,86%	0,11%	0,96%	0,27%	0,82%	0,33%

Table S19: ^{13}C-Excess of sugars obtained after hydrolysis in *Fth*, *Fno* and F-W12 during the exponential growth phase in medium T with the addition of 11 mM [U-^{13}C$_6$]glucose. Mean values and standard deviations are based on two biological replicates with three technical replicates each.

	Fth		*Fno*		*F. W12*	
	Mean	SD	Mean	SD	Mean	SD
Glucose in glycogen	12,75%	3,46%	8,73%	1,78%	7,60%	0,92%
Glucosamine	9,74%	1,18%	9,88%	2,44%	4,47%	0,75%

Table S20: ^{13}C-Excess of sugars obtained after hydrolysis in *Fth*, *Fno* and F-W12 during the post exponential/late exponential growth phase in medium T with the addition of 11 mM [U-^{13}C$_6$]glucose. Mean values and standard deviations are based on two biological replicates with three technical replicates each.

	Fth		*Fno*		*F. W12*	
	Mean	SD	Mean	SD	Mean	SD
Glucose in glycogen	11,17%	0,84%	6,75%	0,73%	7,27%	0,92%
Glucosamine	6,69%	0,26%	5,63%	0,38%	5,08%	0,46%

Table S21: ^{13}C-Excess of sugars obtained after hydrolysis in *Fth*, *Fno* and F-W12 during the stationary growth phase in medium T with the addition of 11 mM [U-^{13}C$_6$]glucose. Mean values and standard deviations are based on two biological replicates with three technical replicates each.

	Fth		*Fno*		*F. W12*	
	Mean	SD	Mean	SD	Mean	SD
Glucose in glycogen	9,11%	0,50%	10,41%	0,87%	6,98%	0,48%
Glucosamine	3,07%	0,50%	9,00%	4,67%	4,36%	3,46%

Table S22: ^{13}C-Excess of sugars obtained after hydrolysis in *Fth*, *Fno* and F-W12 during the exponential growth phase in medium T with the addition of 25 mM [U-^{13}C$_3$]glycerol. Mean values and standard deviations are based on two biological replicates with three technical replicates each.

	Fth		*Fno*		*F. W12*	
	Mean	SD	Mean	SD	Mean	SD
Glucose in glycogen	0,59%	0,13%	4,97%	1,90%	2,68%	1,68%
Glucosamine	1,37%	0,16%	4,66%	0,35%	8,07%	0,41%

Table S23: ^{13}C-Excess of sugars obtained after hydrolysis in *Fth*, *Fno* and F-W12 during the post exponential/late exponential growth phase in medium T with the addition of 25 mM [U-^{13}C$_3$]glycerol. Mean values and standard deviations are based on two biological replicates with three technical replicates each.

	Fth		*Fno*		*F. W12*	
	Mean	SD	Mean	SD	Mean	SD
Glucose in glycogen	0,24%	0,07%	2,23%	1,53%	4,84%	4,88%
Glucosamine	1,15%	0,14%	1,82%	0,24%	2,22%	0,26%

Table S24: ^{13}C-Excess of sugars obtained after hydrolysis in *Fth*, *Fno* and F-W12 during the stationary growth phase in medium T with the addition of 25 mM [U-^{13}C$_3$]glycerol. Mean values and standard deviations are based on two biological replicates with three technical replicates each.

	Fth		*Fno*		*F. W12*	
	Mean	SD	Mean	SD	Mean	SD
Glucose in glycogen	0,10%	0,07%	0,91%	0,69%	4,20%	4,59%
Glucosamine	0,85%	0,09%	0,91%	0,06%	2,22%	2,13%

Table S25: ^{13}C-Excess of sugars obtained after hydrolysis in *Fth*, *Fno* and F-W12 during the exponential growth phase in medium T with the addition of 5 mM [2,3-^{13}C$_2$]alanine. Mean values and standard deviations are based on two biological replicates with three technical replicates each.

	Fth		*Fno*		*F. W12*	
	Mean	SD	Mean	SD	Mean	SD
Glucose in glycogen	0,03%	0,10%	0,67%	0,86%	0,07%	0,12%
Glucosamine	1,18%	0,42%	0,90%	0,33%	1,12%	0,18%

Table S26: ^{13}C-Excess of sugars obtained after hydrolysis in *Fth*, *Fno* and F-W12 during the ost exponential/late exponential growth phase in medium T with the addition of 5 mM [2,3-^{13}C$_2$]alanine. Mean values and standard deviations are based on two biological replicates with three technical replicates each.

	Fth		*Fno*		*F. W12*	
	Mean	SD	Mean	SD	Mean	SD
Glucose in glycogen	0,20%	0,13%	0,02%	0,09%	0,09%	0,09%
Glucosamine	0,98%	0,20%	1,18%	0,09%	1,08%	0,40%

Table S27: ^{13}C-Excess of sugars obtained after hydrolysis in *Fth, Fno* and F-W12 during the stationary growth phase in medium T with the addition of 5 mM [2,3-^{13}C$_2$]alanine. Mean values and standard deviations are based on two biological replicates with three technical replicates each.

	Fth		*Fno*		*F. W12*	
	Mean	SD	Mean	SD	Mean	SD
Glucose in glycogen	0,06%	0,05%	0,10%	0,05%	0,08%	0,09%
Glucosamine	1,45%	0,17%	1,08%	0,18%	0,96%	0,21%

Table S28: ^{13}C-Excess, isotopologue profile and concentration of alanine in the supernatant after growth of *Fno* in medium T for 15 h. After 5 h of growth 25 mM [U-^{13}C$_3$]glycerol were added to the medium. Mean values and standard deviations are based on two biological replicates with three technical replicates each.

Labeling profile Alanine			Concentration Alanine [mM]	
	Mean	SD	Mean	SD
^{13}C-Excess	27,25%	1,47%	8,58	2,58
M+1	0,89 %	0,10%		
M+2	1,82 %	0,34%		
M+3	25,73 %	1,33%		